doi:10.1017/S1431927613009458
Microsc. Microanal. 19 (Suppl 2), 2013

Effect of Atomic Structure on the Performance of Lithium-rich Layered Oxides: An Aberration-Corrected STEM and D-STEM Investigation

K. Jarvis[1], C-C. Wang [1], A. Manthiram[1], P.J. Ferreira[1].

[1.] Materials Science and Engineering Program, The University of Texas at Austin, Austin, TX, 78712.

The $Li[Li_{1/3-2x/3}Mn_{2/3-x/3}Ni_x]O_2$ ($0 < x \leq ½$) series shows promise as a candidate for Li-ion battery cathodes due to its high capacity. The charging curves of these materials contain two regions, a sloping region and a plateau region. The sloping region is associated with the oxidation of Ni [1,2], while the plateau region is attributed to the oxidation of O, which is facilitated by the excess of Li [1,2]. However, the factors effecting oxidation loss are not fully understood, in particular the role of the atomic structure. To address this issue, we have studied the atomic structure of four compositions, ranging from no excess Li (x = 0.5) to an excess Li of x = 0.2, prepared by two different methods, EDTA and OH. These samples were heat-treated at 900°C for 12 h and observed with aberration-corrected STEM and diffraction-STEM (D-STEM). D-STEM, developed in our lab, was used to map particles with a 1-2 nm resolution [3]. As expected, the charging curves of these materials show a decrease in the sloping region and an increase in the plateau region as the Li content increases.

Aberration-corrected STEM (Fig. 1) and D-STEM (Fig. 2) reveal that i) several atomic arrangements may exist within each particle and ii) the number and type of arrangements depend on composition. In particular, we found two well-known structures, $R\bar{3}m$ and *C2/m*, viewed down the $[120]_T$ (Figs. 1a, 1e, 2a, 2e) and $[100]_M$ (Figs. 1d, 1h, 2d and 2h) zone axes, respectively. We also observed the $R\bar{3}m$ along the $[12\bar{1}]_T$ zone axis (Figs. 1i-1k,1m-1o, 2i-2k and 2m-2o) and the *C2/m* structure along the $[001]_M$ zone axis (Figs. 1l, 1p, 2l and 2p). A fifth arrangement shows a structure similar to a NaCl structure viewed along the $<11\bar{2}>_{NaCl}$ zone axis (Figs. 1q-1w and 2q-2x). The last two arrangements (Figs. 1x-1z, 2y-2ac and Figs. 1aa-1ad, 2ad-2ai) require a more in-depth analysis, which we discuss below.

Consider the layered oxides as a NaCl structure in which the M and Li layers alternate on the Na $\{111\}_{NaCl}$ layers and O occupies the Cl sites. The four $\{111\}_{NaCl}$ planes of pure NaCl are equivalent; however, due to cation ordering, the four $\{111\}_{NaCl}$ planes in layered oxides are no longer equivalent. Thus, when viewed along a unique zone axis, cation layers ordered on different $\{111\}_{NaCl}$ planes within a single particle produce different atomic arrangements. In fact, the first six of the aforementioned arrangements (Figs. 1a-z and 2a-ac) result from cation layers ordering on different $\{111\}_{NaCl}$ planes. The final arrangement (Figs. 1aa-1ad and 2ad-2ai) results from an overlap along the beam direction of two of the six arrangements discussed above.

This work shows that aberration-corrected STEM images and electron diffraction patterns from Li-layered oxides should be analyzed carefully, because a single phase material may appear multiphase due to cation layers ordering on different $\{111\}_{NaCl}$ planes. Overall, as the amount of Li increases, there is a change from an $R\bar{3}m$ structure at x = 0.5 to a *C2/m* structure at x = 0.2. Compositions in the range $0.2 < x < 0.5$ show both $R\bar{3}m$ and *C2/m* structures. The increase in the *C2/m* phase corresponds to higher oxygen loss and, hence, greater capacity.

References:

[1] Z. Q. Deng and A. Manthiram, The J. of Phys. Chem. **115** (2011), 7097.

[2] Armstrong, A. R. et al., J. Am. Chem. Soc. **128** (2006), 8694.
[3] K. J. Ganesh et al., Microsc. Microanal. **16** (2010), 614.
[4] This work was supported by the Department of Energy, Office of Basic Energy Sciences as part of the Energy Frontier Research Center (EFRC). The aberration-corrected microscopy was supported by a grant from the National Institute on Minority Health and Health Disparities (G12MD007591) from the National Institutes of Health.

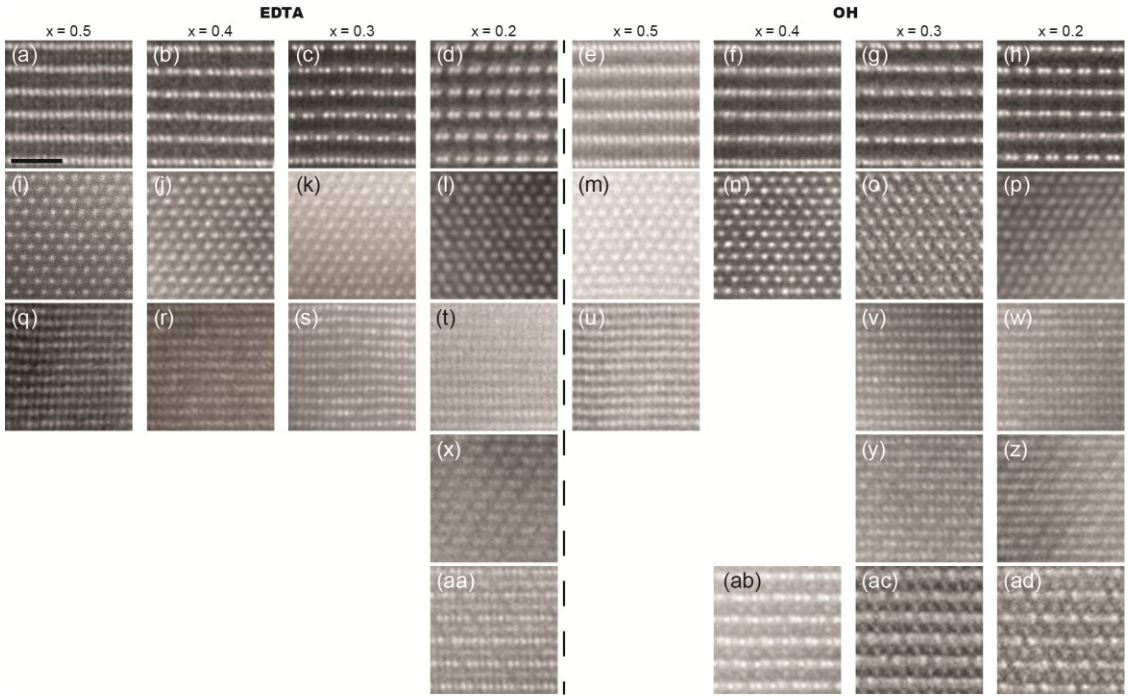

Figure 1. Aberration-corrected STEM images from the $Li[Li_{1/3-2x/3}Mn_{2/3-x/3}Ni_x]O_2$ ($0 < x \leq ½$) series prepared by EDTA (left of dashed line) and OH (right of dashed line) for compositions x = 0.5, 0.4, 0.3, and 0.2 viewed down the $<11\bar{2}>_{NaCl}$ zone axis. The scale bar = 1 nm in (a) applies to all images.

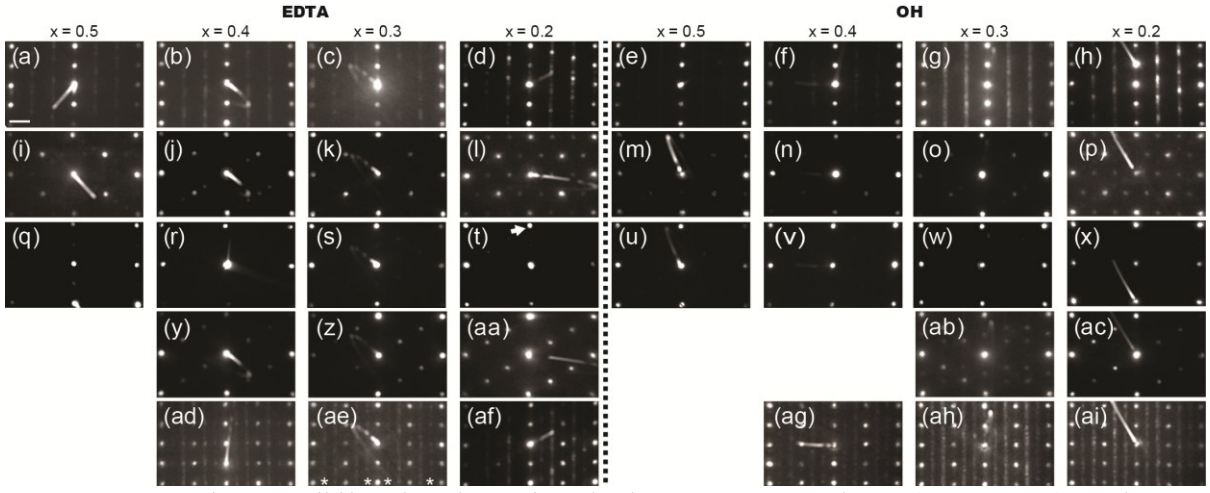

Figure 2. D-STEM electron diffraction from the $Li[Li_{1/3-2x/3}Mn_{2/3-x/3}Ni_x]O_2$ ($0 < x \leq ½$) series prepared by EDTA (left of dashed line) and OH (right of dashed line) for compositions x = 0.5, 0.4, 0.3, and 0.2 viewed down the $<11\bar{2}>_{NaCl}$ zone axis. The scale bar = 2 nm^{-1} in (a) applies to all images. Due to limited space, the patterns have not been indexed. However, each D-STEM pattern matches the FFT expected for the corresponding STEM image in figure 1.

https://doi.org/10.1017/S1431927613009458 Published online by Cambridge University Press